

Article

Stability and Retention of Nanoemulsion Formulations Incorporating Lavender Essential Oil

Konstantina Flekka¹, Virginia D. Dimaki² , Elena Mourelatou³, Konstantinos Avgoustakis¹, Fotini N. Lamari² 
and Sophia Hatziantoniou^{1,*} 

- ¹ Laboratory of Pharmaceutical Technology, Department of Pharmacy, School of Health Sciences, University of Patras, 26 504 Patras, Greece; corn_flek@yahoo.com (K.F.); avgoust@upatras.gr (K.A.)
- ² Laboratory of Pharmacognosy and Chemistry of Natural Products, Department of Pharmacy, School of Health Sciences, University of Patras, 26 504 Patras, Greece; virnadimaki@gmail.com (V.D.D.); flam@upatras.gr (F.N.L.)
- ³ Pharmacy Program, Department of Health Sciences, School of Life and Health Sciences, University of Nicosia, 2417 Nicosia, Cyprus; mourelatou.e@unic.ac.cy
- * Correspondence: sohatzi@upatras.gr

Abstract: Lavender essential oil (LEO) is applied topically for its soothing properties, serving not only as an antiseptic in wound care but also as an insect repellent. This study investigates the impact of carrier systems on LEO encapsulation, stability, and release kinetics for potential skincare applications. The LEO carrier impact on skin hydration and barrier function was also evaluated. Conventional emulsions (CEs) and nanoemulsions (NEs) with (CEs and NELs, respectively) and without LEO incorporation were analyzed for physicochemical properties, stability, and release mechanisms. The droplet size distribution and ζ -potential remained consistent in both CE and NEL, showing the minimal influence of LEO on those parameters. NE and NEL exhibited enhanced stability and higher LEO retention compared to CE and CEL ($37.38 \text{ mg/mL} \pm 0.48 \text{ mg/mL}$ and $50.96 \text{ mg/mL} \pm 2.00 \text{ mg/mL}$, respectively, $p < 0.05$), suggesting NE as a superior carrier system for LEO delivery. NEL retained LEO over 60 days at 4°C without a significant reduction while CEL showed a notable reduction of $94.93\% \pm 0.08\%$. Release kinetics analysis showed zero-order release kinetics of LEO from both CEL and NEL (R^2 : 0.973 and 0.952, respectively), revealing a diffusion-based mechanism, particularly evident in NE formulations, supporting the controlled and sustained release of LEO constituents. NEL also promoted quicker skin barrier repair and enhanced skin hydration, sustaining effects for up to 120 min post application, surpassing CEL's performance. These findings contribute to understanding the carrier system effects on LEO delivery and underscore NE as a promising vehicle for skincare applications. Further research should explore underlying mechanisms and conduct long-term safety and efficacy studies to fully exploit the therapeutic potential of NE in dermatological applications.



Citation: Flekka, K.; Dimaki, V.D.; Mourelatou, E.; Avgoustakis, K.; Lamari, F.N.; Hatziantoniou, S. Stability and Retention of Nanoemulsion Formulations Incorporating Lavender Essential Oil. *Cosmetics* **2024**, *11*, 65. <https://doi.org/10.3390/cosmetics11030065>

Academic Editor: Christophe Hano

Received: 5 March 2024

Revised: 31 March 2024

Accepted: 22 April 2024

Published: 23 April 2024

Keywords: essential oils; nanoemulsion; emulsion; stability; release; retention

1. Introduction

Essential oils are complex mixtures of a large number of volatile plant secondary metabolites and are widely used in cosmetic and pharmaceutical products [1–4]. The diverse range of compounds, even those present in small quantities, contributes not only to the characteristic aroma but also to the potential biological properties of each essential oil. However, several inherent challenges limit their practical application. The high lipophilicity of essential oils complicates their formulation, and their volatility leads to concentration loss, alterations in sensory attributes, and reduced product performance [5]. Additionally, some constituents are known allergens, necessitating mandatory labeling as per Cosmetic Regulation EC 1223/2009 Annex III, where allergen concentrations exceeding 0.01% in



Copyright: © 2024 by the authors. Licensee MDPI, Basel, Switzerland. This article is an open access article distributed under the terms and conditions of the Creative Commons Attribution (CC BY) license (<https://creativecommons.org/licenses/by/4.0/>).

rinse-off products and 0.001% in leave-on products must be disclosed [6]. Volatility may also lead to inaccuracies in label claims.

Lavender essential oil (LEO) is obtained from the flowering tops of *Lavandula angustifolia* Mill. It finds extensive application in cosmetics under the INCI name Lavandula angustifolia oil (CAS numbers 8000-28-0, 90063-37-9; EC number 289-995-2), and holds significant value in pharmaceuticals and the food industry [7]. LEO is renowned for its sedative, antispasmodic, and anti-inflammatory properties. Its calming effects make it suitable for relieving headache and indigestion, whereas its ability to promote cell growth makes it suitable for topical use in skin regeneration [8]. Traditionally, lavender oil served as an antiseptic for wound healing, burns, and insect bites. Furthermore, it exhibits insect-repellent properties, finding utility in veterinary applications for the prevention of fleas and other animal parasites [9,10].

LEO demonstrates remarkable efficacy against various bacteria, including antibiotic-resistant strains like multidrug-resistant microbes [11,12]. Moreover, LEO exhibits antifungal activity against pathogens like *Candida albicans* [13,14]. The composition and relative concentration of its ingredients play a pivotal role in determining LEO's antimicrobial activity [15].

Nanoemulsions (NEs) are oil-in-water dispersions with droplets typically around 100 nm in size, primarily formed through high-shear-induced rupture. The small droplet size and the steric stabilization with appropriate surface functionalization confer long-term stability [16]. NEs are characterized as thermodynamically stable systems, resisting phenomena like creaming, sedimentation, flocculation, or coalescence observed in conventional emulsions. They exhibit low viscosity and a large surface area [17].

NEs distinguish themselves from conventional emulsions due to their small droplet size, high kinetic stability, and optical transparency [18]. Their primary advantage stems from the high surface-to-volume ratio of dispersed phase droplets, which enhances the solubility of sparingly soluble drugs and the skin penetration of incorporated ingredients [2]. They also protect the incorporated molecules from hydrolysis and enzymatic degradation, making them ideal carriers for sensitive ingredients, extending chemical stability and increasing bioavailability [2,19]. This ensures stability, minimizes toxicity during use, and limits the volatility of volatile components, preserving both the activity and sensory attributes of the product [5,20]. Recently, the use of nanoemulsions incorporating LEO has gained great interest due to their enhanced wound-healing properties [21,22].

The primary aim of this research is to investigate the influence of the carrier on the retention of LEO. Additionally, this study seeks to design and prepare nanoemulsions incorporating LEO, characterize them physicochemically, assess their stability, and evaluate their capacity to retain the essential oil. To achieve these objectives, we prepared both conventional emulsions and nanoemulsions, with or without LEO incorporation. We measured the size distribution of dispersed-phase droplets and quantified the content of incorporated LEO. The colloidal stability was studied, and the mechanism of essential oil component release was investigated. To the best of our knowledge, this is the first time that the release kinetics of the essential oil components incorporated in lipid nanoparticles have been studied, allowing for a comparison with conventional emulsions.

2. Materials and Methods

2.1. Materials

Miglyol 812 (Crodamol GTCC (S); Croda, Leek, UK, INCI: caprylic/capric triglycerides), Softisan[®] 154 (Condea, Witten, Germany, INCI: hydrogenated palm oil), Solutol[®] HS 15 (BASF; Ludwigshafen, Germany, INCI: PEG-15-hydroxystearate), Emulmetik[™] 900 (Lucas Meyer Cosmetics, Massy, France, INCI: Lecithin), water for injection (WFI) (Demo S.A., Pharmaceutical Industry, Kryoneri, Attica, Greece), lavender essential oil (CHEMCO by Syndesmos, Acharnai, Greece, INCI: Lavandula Angustifolia Oil).

2.2. Sample Preparation

2.2.1. Preparation of Conventional Emulsions (CEs) and Nanoemulsions (NEs)

Conventional emulsions (CEs) were formulated by melting the lipid phase ingredients, including hydrogenated palm oil, caprylic/capric triglycerides, lecithin, and PEG-15-hydroxystearate, in a 1:2:3:1.44 (*w/w*) ratio. These ingredients were melted at 75–80 °C and then added to purified water, also heated to the same temperature. The mixture was vigorously stirred until it reached room temperature. Each CE preparation was repeated three times.

Nanoemulsions (NEs) were prepared by subjecting CEs to ultrasonication using a probe sonicator (Vibra cell™, Sonics & Materials, Newtown, CT, USA) with an amplitude of 83%. Ultrasonication was performed for four cycles, each lasting 30 s, with vortexing at intervals between cycles until the NE reached room temperature. This process was also repeated three times. Both formulations were allowed to rest for 24 h prior to any measurement.

2.2.2. Preparation of Conventional Emulsions with Lavender Essential Oil (CEs) and Nanoemulsions with Lavender Essential Oil (NELs)

One day after the preparation of CE and NE, lavender essential oil (LEO) was added to each sample and incorporated by vigorous vortexing. The maximum amount of LEO that could be incorporated was determined by adding it drop by drop and observing the point at which oil appeared on the sample's surface.

2.3. Physicochemical Characterization

2.3.1. Droplet Size Distribution of CE and CEL

The droplet size distribution of CE and CEL was determined using Static Light Scattering (Mastersizer S, Malvern Panalytical Ltd., Malvern, UK). One day after preparation, 1 mL of each sample was diluted with WFI until the obscuration fell within the range of 12% to 30%. The droplet size distribution was characterized by measuring the volume-weighted mean ($D[4,3]$) and the uniformity (Span).

2.3.2. Droplet Size distribution of NE and NEL

The droplet size distribution of NE and NEL was assessed using Dynamic Light Scattering (DLS) with a Zetasizer Nano-ZS (Malvern Panalytical Ltd., Malvern, UK). NE and NEL were diluted with WFI (100 µL of sample + 600 µL of WFI) and measurements were conducted at 25 °C by setting the refractive index to 1.333 (water). The average particle size (mean size) and polydispersity index (PDI) were determined.

2.3.3. ζ-Potential Distribution of NE and NEL

The ζ-potential of NE and NEL was measured using Electrophoretic Light Scattering (ELS) with the Zetasizer Nano-ZS (Malvern Panalytical Ltd., Malvern, UK). Sample preparation followed the same procedure as for particle size determination, and measurements were conducted at 25 °C. The average ζ-potential value and width of the distribution were determined based on the Smoluchowski equation.

2.4. Measurement of LEO Incorporation in CEL and NEL

The qualitative and quantitative analysis of LEO, whether free or incorporated into CE and NE, was conducted using Gas Chromatography–Mass Spectrometry (GC-MS). An Agilent 6890N Gas Chromatographer coupled to an Agilent 5975 B mass spectrometer (Agilent Technologies, Inc., Santa Clara, CA, USA) was employed for this analysis. The chromatographic system utilized an HP-5MS non-polar column (30 m × 0.25 mm × 0.25 µm film thickness). Electron impact ionization at 70 eV and helium as a carrier gas at a flow rate of 1 mL/min were employed.

For each sample, 2 mL was diluted with 5 mL of water, and LEO was extracted with 5 mL of hexane through vigorous shaking. The organic phase was collected in a screw-top

glass vial, and this procedure was repeated three times. The collected organic phase (15 mL) was washed with a saturated NaCl solution to remove residual moisture. Any remaining moisture was removed by adding a small quantity of anhydrous Na₂SO₄ while shaking, followed by filtering the organic phase through a paper filter. Subsequently, hexane was removed in vacuo. The extracted LEO was stored at −20 °C until further analysis.

For the GC-MS analysis, octane was used as an internal standard with a concentration of 0.1 mg/mL in the sample (diluted in pentane at 1:25, *v/v*). A 1 µL volume was injected in splitless mode, with the injector temperature set to 300 °C. The initial oven temperature was set to 40 °C and ramped to 80 °C at a rate of 2 °C/min, where it was maintained for 2 min. The temperature was then further increased to 130 °C (at a 4 °C/min rate) and then to 150 °C (at a 2 °C/min rate). Subsequently, the temperature was raised to 260 °C at a rate of 5 °C/min and maintained for 2 min.

The obtained mass spectra were processed using the AMDIS Analysis software (Automated Mass spectral Deconvolution & Identification System v.2.73, NIST Institute). Identification was accomplished by comparing the mass spectra with those in the NIST MS Search v.2.0 spectral library and referencing bibliographic data on the retention index (Retention/Kovats Index). Quantification was achieved through the construction of calibration curves using eucalyptol (>99% purity, Sigma-Aldrich, St. Louis, MA, USA) in concentrations ranging from 0.01 to 12.0 mg/mL and expressed as eucalyptol equivalents.

2.5. Colloidal Stability Assessment

Colloidal stability was evaluated by monitoring the changes in LEO contents using GC/MS and by examining droplet size and ζ-potential distribution using DLS, SLS, or ELS, as appropriate. This assessment was performed as follows:

- i. Centrifugation: samples were subjected to centrifugation at 3000 rpm for 30 min.
- ii. Accelerated aging: samples underwent three consecutive 24 h cycles of storage at 45 °C and 25 °C.
- iii. Storage under various conditions: samples were stored at 4 °C, 25 °C, and 45 °C for a period of 60 days.

Stability was established if no statistically significant changes were detected in the above-mentioned physicochemical parameters. If loss of stability was observed, no further measurements were conducted.

2.6. Release Kinetics of LEO from CEL and NEL

The release mechanism of LEO from CEL and NEL was estimated by fitting data obtained from the release studies to various mathematical models. Linear regression analysis in Microsoft Excel was employed to calculate the regression coefficient (R^2) for each model. The mathematical models examined were zero-order, first-order, Higuchi, Hixson–Crowell, Korsmeyer–Peppas, and Kopcha release kinetic equations, as previously described [23].

2.7. Study of the Effect of CEL and NEL on Skin Parameters

The effect of the topical application of CEL and NEL on the skin was tested in vivo on 10 healthy volunteers using non-invasive techniques [23,24]. Ten men and women between 20 and 60 years were randomly chosen and signed an informed consent form. Skin conditions like burns and wounds, a history of skin allergies or skin disease, the use of medication, or other conditions like pregnancy were exclusion criteria. The volunteers who agreed to participate were instructed to avoid the use of skin care products or washing the skin of the volar forearms where the study would take place. Three squares (3 cm × 3 cm) for each sample were marked on the randomly picked left or right forearm of every volunteer. One additional square was marked and left untreated serving as a control. CEL or NEL was applied on three squares each at a dose of 2 mg/cm².

The Transepidermal Water Loss (TEWL) and skin hydration were monitored using a Tewameter TM 300 (Courage & Khazaka electronic GmbH, Köln Germany) and a Cor-

neometer CM 825 (Courage & Khazaka electronic GmbH, Köln Germany), respectively. The baseline was determined by measuring each parameter at each skin site before any treatment. After the application of the sample, the skin of the first square to which each sample was applied underwent cleaning using gentle tapping with paper tissue after 30 min. Subsequently, measurements of skin parameters (Transepidermal Water Loss (TEWL) or skin hydration) were recorded. This process was then repeated after 60 min for the second square, and again at the 120 min mark for the third square. Throughout the experiment, measurements of skin parameters were taken for the untreated control square at each designated time point. For the estimation of the skin barrier function repair action of CEL and NEL, the skin barrier was disrupted by rubbing the squares with a cotton bud impregnated with acetone. The TEWL was measured after the skin barrier disruption and before the application of the samples. Each measurement was performed in triplicate and the alterations in TEWL and skin hydration over time were calculated. The normalized values were obtained by subtracting the TEWL and skin hydration values of untreated skin from the corresponding ones of the treated skin measured at each time point.

2.8. Statistical Analysis

All measurements were conducted in triplicate whenever possible, and the results are reported as mean values \pm standard deviation (SD). The statistical significance of differences was assessed using Student's *t*-test, with a significance threshold of $p < 0.05$, and data analysis was performed using Microsoft Office 365 Excel 2016 (Redmond, WA, USA).

3. Results

3.1. Droplet Size Distribution of the Dispersed Phase of CE and CEL

To determine the droplet size distribution of CE and CEL, D[4,3] and the uniformity were measured one day after their preparation. Both CE and CEL had similar mean droplet sizes ($16.46 \pm 5.73 \mu\text{m}$, $13.95 \pm 0.91 \mu\text{m}$, respectively, $p > 0.05$) and uniformity (0.27 ± 0.08 , 0.38 ± 0.25 , respectively, $p > 0.05$).

3.2. Droplet Size Distribution and ζ -Potential of the Dispersed Phase of NE and NEL

The distribution of the droplet size and ζ -potential of the dispersed phase of NE and NEL, one day after their preparation, did not differ significantly ($p > 0.05$). NE and NEL mean particle sizes were $103.04 \pm 12.25 \text{ nm}$ and $101.63 \pm 13.82 \text{ nm}$, respectively, while their PDI was 0.22 ± 0.01 and 0.23 ± 0.02 , respectively. The results indicate that the incorporation of LEO did not significantly change the size distribution of the dispersed droplets of both CE and NE (Figure 1).

The ζ -potential and width of NE were $-60.5 \pm 2.8 \text{ mV}$ and $9.45 \pm 1.46 \text{ mV}$, respectively, and for NEL, the ζ -potential was $-71.4 \pm 12.7 \text{ mV}$ and the width was 8.18 ± 0.43 . The ζ -potential and width values were similar ($p > 0.05$) for both NE and NEL (Figure 2).

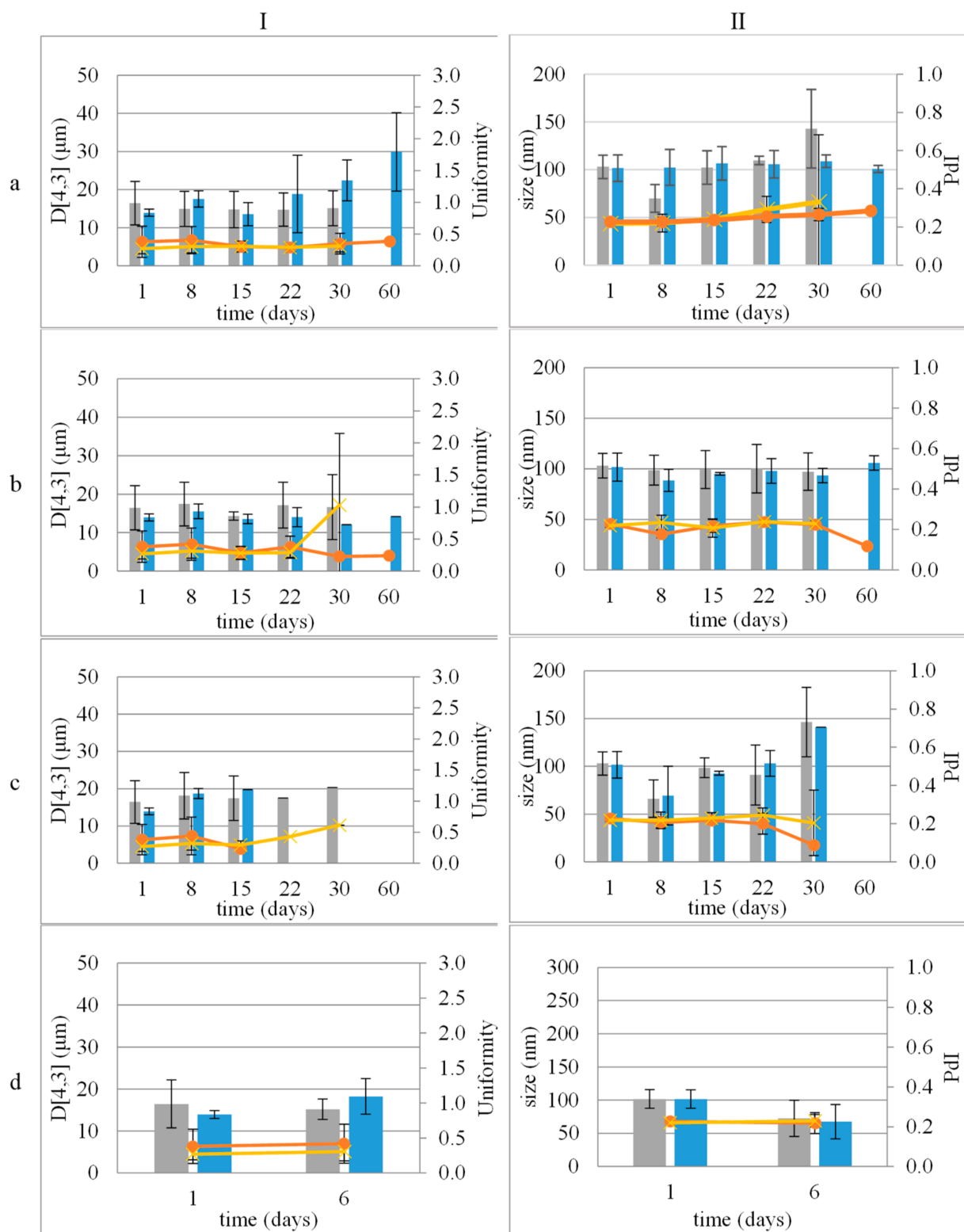


Figure 1. Stability study of emulsions (I) and nanoemulsions (II) during storage at 4 °C (a), 25 °C (b), and 45 °C (c) and accelerated aging (three 24 h circles of storage at 45 °C and 25 °C) (d). Size distribution: mean droplet size of empty (■) or loaded with LEO (■) and uniformity or PdI describing size distribution width of emulsions or nanoemulsions, empty (x) or loaded (●) with LEO, respectively.

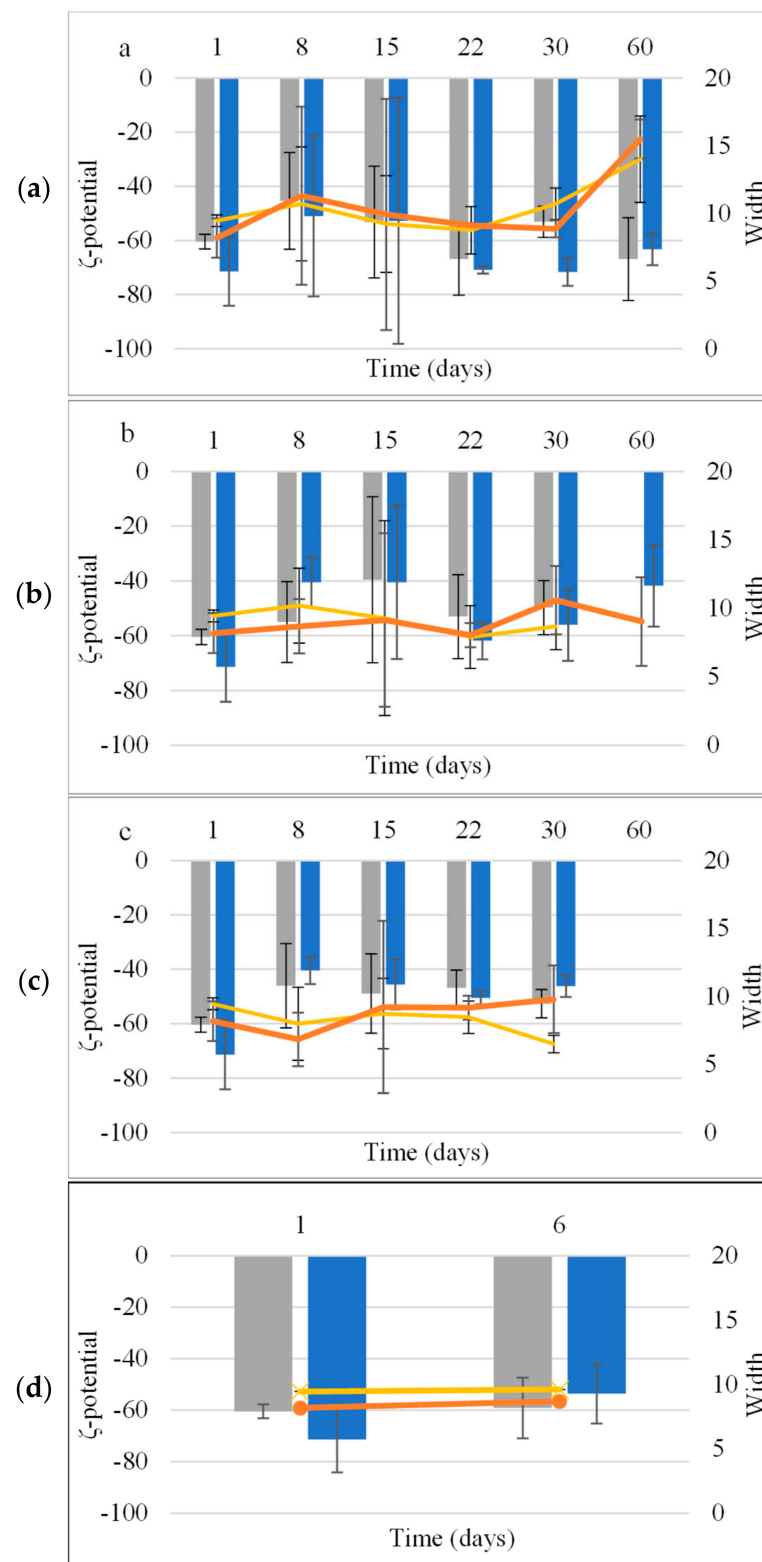


Figure 2. Mean ζ -potential and width of NE (■, x) and NEL (■, ●) during storage at 4 °C (a), 25 °C (b), and 45 °C (c) and accelerated aging (three 24 h cycles of storage at 45 °C and 25 °C) (d).

3.3. LEO Content in CEL and NEL

The analysis of LEO revealed that the main ingredients were linalool (33.19%) and linalool acetate (30.49%) (Table 1). Camphor (7.36%), eucalyptol (5.18%), and borneol (3.6%) were also identified in substantial quantities, while terpinen-4-ol, caryophyllene

oxide, α -terpineol, and isoborneol were found in percentages ranging from 1.42% to 1.19%. Lavandulyl acetate in 0.71% and several other ingredients in traces were also identified.

Table 1. Content (mg/mL) of ingredients of LEO incorporated in CEL (A) and NEL (B) over a period of 60 days after their preparation and storage at 4 °C.

A Components	CEL					
	Time (days)	1	15	30	45	60
eucalyptol		0.440 ± 0.044	0.403 ± 0.025	0.342 ± 0.010	0.220 ± 0.009	0.097 ± 0.001
<i>cis</i> -linalool oxide (furanoid)		0.063 ± 0.001	0.060 ± 0.001	0.055 ± 0.007	0.033 ± 0.006	0.011 ± 0.000
linalool		24.237 ± 0.976	20.610 ± 0.372	17.198 ± 0.069	9.185 ± 0.035	1.276 ± 0.042
camphor		2.893 ± 0.110	2.587 ± 0.064	2.159 ± 0.257	1.171 ± 0.142	0.144 ± 0.005
isoborneol		0.142 ± 0.008	0.130 ± 0.001	0.107 ± 0.001	0.062 ± 0.001	0.020 ± 0.000
borneol		0.342 ± 0.013	0.262 ± 0.006	0.219 ± 0.028	0.143 ± 0.016	0.060 ± 0.001
terpinen-4-ol		0.206 ± 0.004	0.193 ± 0.012	0.165 ± 0.006	0.107 ± 0.019	0.030 ± 0.001
α -terpineol		0.186 ± 0.012	0.164 ± 0.009	0.138 ± 0.004	0.082 ± 0.001	0.027 ± 0.001
linalool acetate		8.760 ± 0.429	6.756 ± 0.378	4.770 ± 0.218	2.485 ± 0.035	0.217 ± 0.004
lavandulyl acetate		0.042 ± 0.001	0.033 ± 0.005	0.029 ± 0.001	0.017 ± 0.001	0.006 ± 0.000
caryophyllene-oxide		0.042 ± 0.002	0.039 ± 0.005	0.028 ± 0.003	0.015 ± 0.001	0.005 ± 0.000
Total		37.355 ± 0.517	31.235 ± 0.075	25.209 ± 0.048	13.517 ± 0.107	1.893 ± 0.055
B Components	NEL					
	Time (days)	1	15	30	45	60
eucalyptol		1.605 ± 0.248	1.385 ± 0.219	0.984 ± 0.255	0.730 ± 0.069	0.481 ± 0.129
<i>cis</i> -linalool oxide (furanoid)		0.096 ± 0.001	0.094 ± 0.002	0.092 ± 0.001	0.092 ± 0.003	0.092 ± 0.003
linalool		31.530 ± 2.995	30.854 ± 2.384	30.053 ± 2.995	27.222 ± 0.322	23.371 ± 0.346
camphor		4.711 ± 0.062	4.700 ± 0.057	4.602 ± 0.062	4.154 ± 0.037	3.706 ± 0.038
isoborneol		0.182 ± 0.010	0.176 ± 0.001	0.181 ± 0.010	0.162 ± 0.004	0.145 ± 0.003
borneol		1.316 ± 0.047	1.149 ± 0.021	1.001 ± 0.027	0.715 ± 0.028	0.408 ± 0.001
terpinen-4-ol		0.271 ± 0.028	0.270 ± 0.029	0.269 ± 0.028	0.254 ± 0.019	0.239 ± 0.007
α -terpineol		0.241 ± 0.019	0.237 ± 0.021	0.225 ± 0.019	0.223 ± 0.019	0.221 ± 0.003
linalyl acetate		12.244 ± 0.584	10.892 ± 0.328	9.531 ± 0.060	7.671 ± 0.004	5.853 ± 0.047
lavandulyl acetate		0.055 ± 0.002	0.052 ± 0.002	0.047 ± 0.000	0.040 ± 0.000	0.033 ± 0.001
caryophyllene-oxide		0.060 ± 0.004	0.055 ± 0.001	0.047 ± 0.003	0.039 ± 0.004	0.031 ± 0.001
Total		52.311 ± 2.603	49.862 ± 2.249	47.032 ± 1.897	41.302 ± 0.381	34.580 ± 0.245

The maximum content of LEO in CEL was significantly smaller ($p < 0.05$) compared to NEL (37.38 ± 0.48 mg/mL and 50.96 ± 2.00 mg/mL, respectively).

The content of each ingredient in CEL and NEL one day after their preparation is summarized in Table 1. The content of all ingredients did not differ significantly between CEL and NEL ($p > 0.05$), except for camphor, borneol, and *cis*-linalool oxide which were higher in NEL ($p < 0.05$).

The major constituents of LEO incorporated in both CEL and NEL one day after preparation were linalool (24.24 ± 0.98 mg/mL, 31.53 ± 3.00 mg/mL, respectively), linalool acetate (8.76 ± 0.43 mg/mL, 12.24 ± 0.58 mg/mL, respectively), camphor (2.89 ± 0.11 mg/mL, 4.71 ± 0.06 mg/mL), eucalyptol (0.44 ± 0.04 mg/mL, 1.60 ± 0.25 mg/mL, respectively), and borneol (0.34 ± 0.01 mg/mL, 1.32 ± 0.05 mg/mL). Other minor LEO constituents

incorporated in CEL and NEL were terpinen-4-ol, α -terpineol, isoborneol, *cis*-linalool oxide (furanoid), lavandulyl acetate, and caryophyllene-oxide.

3.4. Stability Study

3.4.1. Colloidal Stability of Nanocarriers

All samples did not show signs of physical instability after centrifugation, a result that suggests their resistance to mechanical stresses.

Both CE and NE remained stable for 30 days at 4 °C, 25 °C, and 45 °C (Figure 1).

The incorporation of LEO improved the stability of the samples. Both CEL and NEL were stable at 4 °C and 25 °C for 60 days (Figure 1a,b). Storage at 45 °C did not seem to favor the stability of both CEL and NEL, as they remained stable for 15 days and 30 days, respectively (Figure 1c).

The ζ -potential of both NE and NEL remained stable under all tested conditions without any statistically significant differences (Figure 2).

All samples also successfully passed the accelerated aging test (Figures 1d and 2d).

3.4.2. LEO Retention in CEL and NEL

The concentration of LEO incorporated in CEL and NEL as measured 30 days after preparation and storage at 4 °C was 25.21 ± 0.05 mg/mL and 47.03 ± 1.90 mg/mL, respectively. At 60 days, the LEO content in CEL and NEL dropped to 1.89 ± 0.06 mg/mL and 34.58 ± 0.25 mg/mL, respectively (Figure 3a). The reduction in LEO incorporated in CEL, 30 days after preparation, was $32.51 \pm 0.81\%$ ($p = 0.01$) and reached $94.93 \pm 0.08\%$ ($p = 0.004$) at 60 days (Figure 3b). The LEO content in NEL was 47.03 ± 1.9 mg/mL at 30 days and 34.58 ± 0.24 mg/mL at 60 days after preparation and storage at 4 °C. This reduction was not statistically significant ($p > 0.05$) (Figure 3).

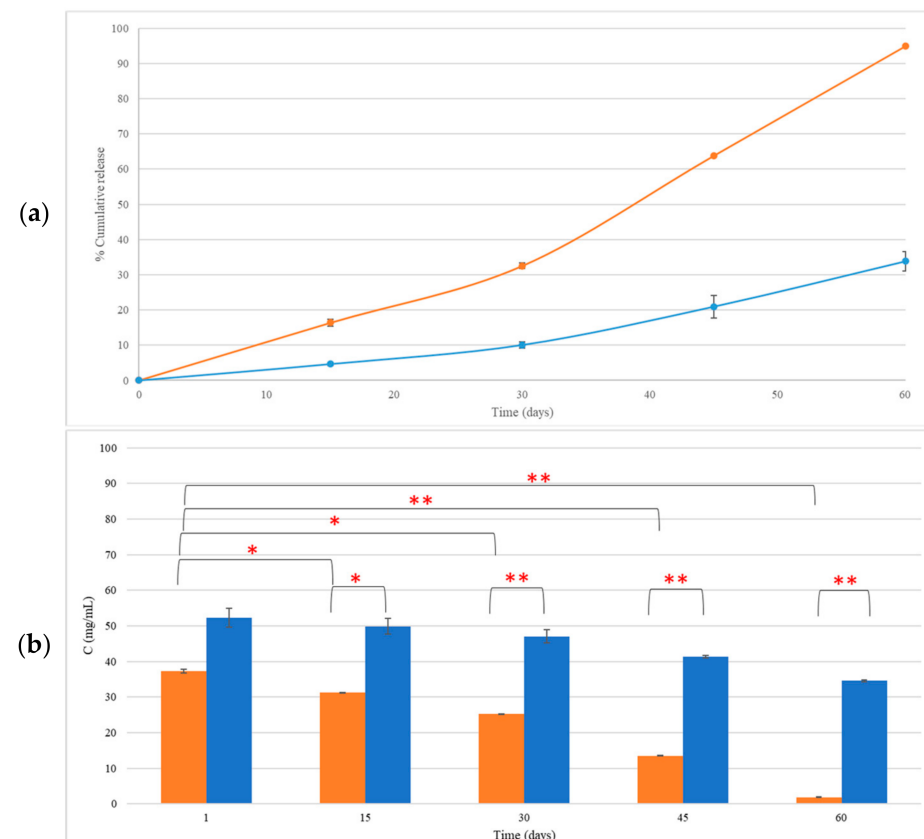


Figure 3. The release rate (a) and concentration of LEO incorporated in CEL (■) and NEL (■) (b) over a period of 60 days after storage. * $p < 0.05$, ** $p < 0.005$.

After 30 days of storage of CEL, the major component that was significantly reduced ($p < 0.05$) was linalyl acetate ($45.5 \pm 0.2\%$), while at 60 days, all LEO components except eucalyptol were significantly reduced from $82.59 \pm 0.38\%$ for borneol to $97.52 \pm 0.17\%$ for linalyl acetate ($p < 0.05$, Figure S1). At 30 days of NEL storage, only eucalyptol and borneol were significantly reduced ($39.23 \pm 6.45\%$, $23.95 \pm 0.67\%$, respectively, $p < 0.05$) in NEL (Figure S1b), while at 60 days, only camphor, borneol, and linalyl acetate were further reduced by $21.31 \pm 0.23\%$, $68.99 \pm 1.20\%$, and $52.15 \pm 2.66\%$ (Table S1).

Comparing LEO compositions incorporated in CEL and NEL 60 days after storage at 4°C revealed that only the composition of eucalyptol was similar in both carriers. The composition of all other ingredients differed significantly ($p < 0.05$).

3.5. Release Mechanism of Ingredients of LEO Incorporated in CEL and NEL

The fitting of the release data on several mathematical models revealed that the release kinetics of LEO ingredients from CEL were effectively described by both the zero-order and Korsmeyer–Peppas models. The zero-order model exhibited R^2 ranging from 0.889 to 0.999 for all ingredients, while the R^2 values for the Korsmeyer–Peppas model, particularly for linalool, borneol, α -terpineol, linalool acetate, and lavandulyl acetate, exceeded 0.9, indicating a highly satisfactory fitting (Table 2a).

Similarly, the release kinetics of most LEO ingredients (eucalyptol, borneol, linalool acetate, lavandulyl acetate, and caryophyllene-oxide) from NEL were found to follow the zero-order model with R^2 values surpassing 0.989 (Table 2b). Additionally, the Korsmeyer–Peppas model demonstrated a satisfactory fit for eucalyptol, *cis*-linalool oxide (furanoid), borneol, linalool acetate, and caryophyllene-oxide with R^2 values exceeding 0.9 (Table 2b).

However, for certain compounds such as linalool, camphor, isoborneol, and α -terpineol, the R^2 values were less than 0.880, indicating poor fitting to all tested models (Table 2b).

Notably, the release exponent (n) of the Korsmeyer–Peppas model for all constituents of either CEL or NEL was below 0.35, indicative of Fickian diffusion release.

Furthermore, when considering LEO as a single entity incorporated in both CEL and NEL, the release kinetics followed a zero-order pattern, with higher R^2 values (0.973 and 0.952, respectively), indicating a superior fit compared to other models.

3.6. Skin Hydration and TEWL Alterations

The effects of NEL and CEL on skin hydration, compared to untreated skin sites, were investigated. Skin hydration levels were evaluated initially at baseline ($t = 0$ h) and subsequently at various time points post-application. Our results indicate that at $t = 0$ h, there were no significant differences in skin hydration among the treatment groups (NEL: 26.9 ± 5.5 units, CEL: 25.6 ± 5.0 units, untreated: 27.0 ± 5.3 units, $p > 0.05$, Table S2). However, thirty minutes after application, both NEL and CEL formulations exhibited a significant increase in skin hydration compared to baseline (NEL: 36.4 ± 3.2 units, CEL: 34.7 ± 3.8 units, Table S2). This increase was sustained at 1 h and 2 h post-application for both formulations ($p < 0.05$). Notably, NEL demonstrated a greater enhancement in skin hydration compared to CEL at 1 h (9.6 ± 4.6 units vs. 7.6 ± 3.6 units, $p < 0.05$), a difference that persisted for at least 2 h (6.7 ± 4.3 units for NEL vs. 2.4 ± 2.2 units for CEL, $p < 0.05$) (Figure 4a). Normalized skin hydration values, obtained by subtracting the values of untreated sites from the treated ones for each sample, corroborated these findings at both time points (Figure 4b).

Table 2. a. Fitting in mathematical models of the release data of LEO ingredients incorporated in CEL. b. Fitting in mathematical models of the release data of LEO ingredients incorporated in NEL.

Kinetic Model	Para-meter	Eucalyptol	<i>cis</i> -Linalool Oxide (furanoid)	Linalool	Camphor	Isoborneol	Borneol	Terpinen-4-ol	α -Terpineol	Linalool Acetate	Lavandulyl Acetate	Caryophyllene-Oxide	LEO
a													
Zero-order	R ²	0.947	0.889	0.960	0.940	0.951	0.991	0.928	0.957	0.999	0.975	0.972	0.973
	K ₀	0.001	0.001	0.001	0.001	0.001	0.001	0.001	0.001	0.001	0.001	0.001	0.001
First-order	R ²	0.040	0.050	0.065	0.072	0.060	0.019	0.007	0.047	0.078	0.031	0.080	0.066
	K ₁	0.000	0.000	0.000	0.000	0.000	0.000	0.000	0.000	0.000	0.000	0.000	0.000
Higuchi	R ²	0.758	0.671	0.790	0.747	0.763	0.900	0.722	0.782	0.899	0.849	0.805	0.817
	K _H	0.243	0.248	0.296	0.293	0.271	0.261	0.267	0.267	0.318	0.271	0.291	0.299
Hixson–Crowell	R ²	0.617	0.638	0.634	0.646	0.629	0.587	0.640	0.618	0.627	0.601	0.635	0.631
	K _{HC}	0.000	0.000	0.000	0.000	0.000	0.000	0.000	0.000	0.000	0.000	0.000	0.000
Korsmeyer–Peppas ¹	R ²	0.875	0.787	0.940	0.895	0.873	0.986	0.799	0.924	0.988	0.973	0.827	0.950
	K _{KP}	1.079	1.096	1.056	1.074	1.083	1.003	1.103	1.062	1.015	1.034	1.010	1.052
	n	0.297	0.272	0.328	0.314	0.307	0.344	0.291	0.316	0.339	0.337	0.318	0.335
Kopcha	R ²	0.171	0.053	0.349	0.174	0.158	0.820	0.070	0.295	0.680	0.668	0.128	0.423
	A	0.059	0.036	0.101	0.071	0.063	0.157	0.043	0.083	0.162	0.138	0.064	0.112
	B	0.000	0.000	0.000	0.000	0.000	0.000	0.000	0.000	0.000	0.000	0.000	0.000
	A/B	195.67	119.00	335.00	238.00	211.00	786.50	108.25	277.67	539.33	692.00	160.00	374.00
b													
Zero-order	R ²	0.989	0.771	0.880	0.852	0.794	0.947	0.831	0.870	0.994	0.963	0.995	0.952
	K ₀	0.001	0.000	0.000	0.000	0.000	0.001	0.000	0.001	0.001	0.001	0.001	0.000
First-order	R ²	0.017	0.771	0.008	0.004	0.034	0.011	0.026	0.140	0.000	0.002	0.000	0.008
	K ₁	0.000	0.000	0.000	0.000	0.000	0.000	0.000	0.000	0.000	0.000	0.000	0.000
Higuchi	R ²	0.908	0.928	0.662	0.613	0.591	0.823	0.600	0.873	0.872	0.801	0.874	0.773
	K _H	0.235	0.014	0.075	0.063	0.057	0.217	0.034	0.030	0.168	0.127	0.159	0.104
Hixson–Crowell	R ²	0.583	0.771	0.582	0.620	0.570	0.591	0.582	0.539	0.572	0.576	0.572	0.573
	K _{HC}	0.000	0.000	0.000	0.000	0.000	0.000	0.000	0.000	0.000	0.000	0.000	0.000
Korsmeyer–Peppas ¹	R ²	0.936	0.997	0.568	0.156	0.354	0.945	0.172	0.636	0.927	0.833	0.909	0.799
	K _{KP}	1.086	1.003	1.177	1.033	1.133	1.051	1.228	1.107	1.085	1.122	1.095	1.125
	n	0.346	0.123	0.206	0.151	0.168	0.307	0.111	0.161	0.313	0.276	0.306	0.255
Kopcha	R ²	0.525	0.975	0.075	0.000	0.187	0.468	0.018	0.397	0.594	0.306	0.509	0.284
	A	0.108	0.018	0.013	0.001	0.018	0.086	0.003	0.015	0.077	0.040	0.067	0.032
	B	0.000	0.000	0.000	0.000	0.000	0.000	0.000	0.000	0.000	0.000	0.000	0.000
	A/B	538.50	17,800.00	138.89	6.00	354.00	431.00	77.50	490.00	772.00	403.00	336.50	318.00

¹ Calculated for release up to 60%.

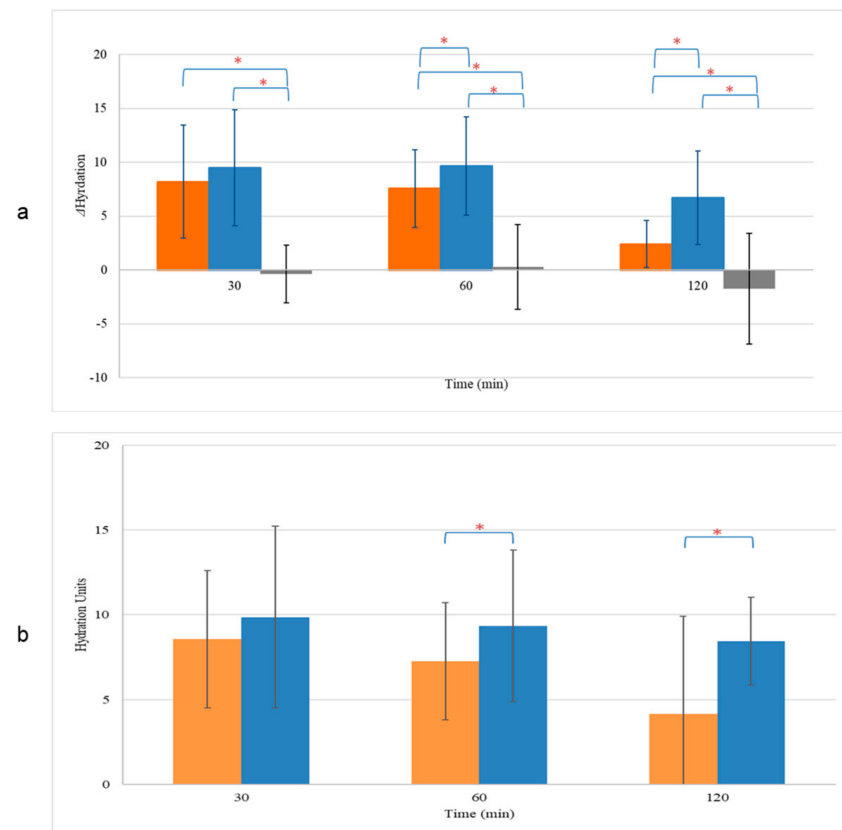


Figure 4. Hydration change (a) and normalized values (b) of skin treated with CEL (■) and NEL (■) or left untreated (■). * $p < 0.05$.

Furthermore, we investigated the effects of NEL and CEL on skin barrier repair by monitoring the restoration of Transepidermal Water Loss (TEWL) after inducing barrier disruption and comparing it to untreated skin. TEWL measurements of the intact skin were comparable across all skin sites (NEL: 6.4 ± 2.3 g/h/m², CEL: 6.8 ± 2.5 g/h/m², untreated: 6.5 ± 1.8 g/h/m², $p > 0.05$, Table S3). Following barrier disruption, TEWL significantly increased compared to baseline values ($p < 0.05$), with similar increases observed for all treatment sites (NEL: 10.1 ± 0.9 g/h/m², CEL: 9.9 ± 1.2 g/h/m², untreated: 10.5 ± 2.6 g/h/m², $p > 0.05$, Table S3). Notably, only the application of NEL led to a significant reduction in TEWL (Δ TEWL) compared to untreated skin, with this effect becoming more pronounced over time (Figure 5a). At 30 min, the Δ TEWL of NEL was -2.4 ± 1.8 g/h/m², while at 2 h, Δ TEWL was -3.7 ± 0.5 g/h/m², indicating full recovery of the skin barrier as TEWL approached baseline values (TEWL of NEL at 2 h: 6.3 ± 1.4 g/h/m², $p > 0.05$). In contrast, CEL application did not significantly affect skin barrier repair compared to untreated skin ($p > 0.05$). The normalized TEWL values, obtained by subtracting the TEWL values of untreated sites from those of treated ones for each sample, demonstrated that NEL application accelerated barrier repair at all time points (Figure 5b).

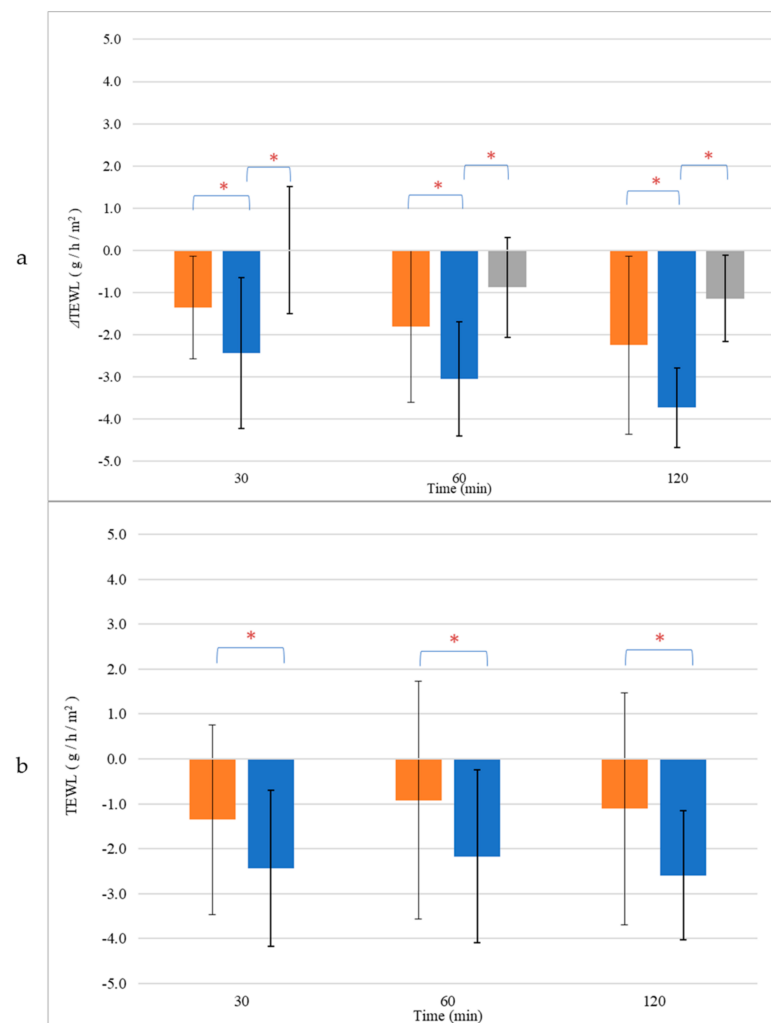


Figure 5. Transepidermal Water Loss (TEWL) change (a) and normalized values (b) of skin treated with CEL (■) and NEL (■) or left untreated (■). * $p < 0.05$.

4. Discussion

The present study aimed to evaluate the impact of the carrier on the concentration of encapsulated LEO and its retention. The physicochemical characteristics (droplet size distribution, ζ -potential, and LEO content), the stability over time, and the release kinetics of LEO constituents in conventional emulsions (CEs) and nanoemulsions (NEs) with and without LEO incorporation (CELs and NELs) were evaluated.

The droplet size distribution of CE and CEL revealed no significant differences in mean droplet size and uniformity, indicating that the incorporation of LEO did not significantly alter the size distribution. This suggests that LEO had minimal influence on the droplet characteristics in both emulsions. Similarly, the droplet size distribution and ζ -potential of NE and NEL remained consistent, with no significant variations after LEO incorporation. This further demonstrates that LEO did not have a substantial impact on the size distribution or surface charge of the dispersed phase in both NE and NEL. Furthermore, the high absolute value of the ζ -potential of NE is indicative of long-term stability.

The analysis of LEO content indicated a higher LEO content in NEL compared to CEL immediately after preparation. The primary LEO constituents, such as linalool, linalool acetate, camphor, eucalyptol, and borneol, showed comparable concentrations in both formulations, with only differences observed in eucalyptol and *cis*-linalool oxide in favor of NEL. Although these minor ingredients may alter several characteristics of essential oils

like sensorial properties and pharmacological activity [25,26], these findings suggest that the droplet size does not significantly affect the incorporation of LEO and its composition.

Colloidal stability assessments revealed that both CE and NE remained stable at different temperatures (4 °C, 25 °C, and 45 °C) for 30 days, with no signs of physical instability. Notably, the incorporation of LEO, resulting in CEL and NEL, enhanced the stability of the emulsions. CEL and NEL demonstrated stability at lower temperatures (4 °C and 25 °C) for longer durations compared to storage at 45 °C, which appeared to affect the stability of both formulations. Both CEL and NEL showed signs of phase separation after storage at 45 °C for 15 and 30 days, respectively. The absence of a longer-term stability of CEL and NEL at the relatively high temperature of 45 °C may be attributed to the increased coalescence frequency with increasing temperature, which has been associated with the change in viscosity at higher temperatures triggering a stronger perturbation in the thin aqueous film separating the droplets [27]. The evolution of ζ -potential values of NE and NEL with storage time at the different temperatures tested followed the respective pattern of droplet size and did not change significantly with storage time at all three temperatures tested for the storage time periods where the nanoemulsions kept their physical stability (did not show signs of phase separation), and it was possible to measure the ζ -potential of the nanoemulsions. The ζ -potential of NEL did not change significantly after 60 days of storage at 4 and 25 °C, indicating NEL physical stability during storage for at least this time period (60 days) under fridge and room conditions [28].

The concentration of LEO incorporated in CE and NE was measured over time. LEO in CEL was gradually reduced over time. Particularly within the first 30 days, about 33% of LEO was lost, and after 60 days, CEL showed a substantial reduction in LEO content, which reached about 95%. All constituents (major and minor) of LEO incorporated in CEL noted significant decreases after 60 days of storage.

Notably, NEL exhibited a statistically non-significant change in LEO content up to 60 days after preparation, indicating its superior ability to retain LEO compared to CEL. The observed change in LEO content was more noticeable between the 30- and 60-day storage periods at 4 °C, particularly evident in the case of the CEL. Although not statistically significant, this phenomenon coincided with a trend of increasing droplet size in CEL over time, as depicted in Figure 1a (I). Small fluctuations in average droplet size may suggest a degree of instability within the emulsion, potentially leading to the leakage of contents over time. This gradual accumulation of leakage could account for the significant difference observed in LEO content between the 30- and 60-day time points (Figures 4 and S1). Further investigation into this phenomenon is warranted to fully elucidate its underlying mechanisms and implications.

The release mechanisms of LEO constituents were assessed, for both CEL and NEL. The best fit for most LEO ingredients incorporated in CE and NEL were as follows:

- i. The zero-order model that describes the release of incorporated ingredients as a function of time, at a constant rate that is independent of its concentration [29].
- ii. The Korsmeyer–Peppas model that is employed to characterize the release of incorporated ingredients in systems where non-Fickian mechanisms occur [30]. This model proves especially valuable in situations where the release mechanism is not known or when multiple types of drug release phenomena occur. This model is most suitable for analyzing the initial 60% of the release curve [29,31].

In all cases, the release exponent n of the Korsmeyer–Peppas model was <0.35 , indicating a Fickian diffusion release [32,33]. This suggests that the release of LEO constituents follows a diffusion-based mechanism. The Korsmeyer–Peppas model is not suitable for releases over 60% [30]. The release from CEL was well above this limit, so the fitting of the release profile of LEO constituents from it may not be considered accurate. The next best fitting was the zero-order model for all LEO constituents incorporated in CEL.

In our study, we also evaluated the effects of NEL and CEL formulations on skin hydration and barrier repair as characterized by TEWL. Both formulations led to significant increases in skin hydration levels, sustained for at least 2 h post application. However,

NEL demonstrated a greater enhancement in skin hydration compared to CEL, suggesting differences in their hydrating potential. The enhanced skin hydration effect of NEL in comparison to CEL has been previously reported [34]. Furthermore, while both formulations showed similar increases in TEWL post-barrier disruption, only NEL significantly reduced TEWL compared to untreated skin, indicating accelerated barrier repair. These results are in accordance with recent research concerning the interaction of LEO on skin characteristics [35]. According to the results of Infante et al., LEO was found to improve the skin barrier with minimum skin penetration, despite the fact its main ingredient is linalool, a known penetration enhancer [35,36].

Our findings suggest that NEL may offer distinct advantages in promoting both hydration and barrier function, highlighting its potential as a promising ingredient in skincare formulations aimed at enhancing skin hydration and facilitating barrier repair.

Further investigations into the underlying mechanisms driving these effects, as well as long-term safety and efficacy studies, are warranted to fully elucidate the therapeutic potential of NEL in dermatological applications.

5. Conclusions

In this study, we explored the impact of carrier systems on lavender essential oil (LEO) encapsulation, stability, and release kinetics. The incorporation of LEO into conventional emulsions (CEs) and nanoemulsions (NEs) had minimal influence on the physical properties of the emulsions, such as droplet size distribution and ζ -potential. However, the incorporation of LEO in nanoemulsions (NELs) significantly improved the stability of NEL and the loading percentage and retention of LEO compared to conventional emulsions (CEs). The release kinetics revealed diffusion-based mechanisms for LEO constituents in both formulations. In addition, our study investigated the effects of NE and CE on skin hydration and barrier function. We observed distinct advantages of NEL over CEL in promoting hydration and accelerating barrier repair, highlighting the potential of NE as a promising carrier of LEO and ingredient in skincare formulations.

These results underline the potential of LEO-incorporated nanoemulsions for enhanced stability and controlled release, with implications for applications in cosmetics and pharmaceuticals. Further research can focus on optimizing LEO delivery and tailoring emulsion formulations for specific applications.

Supplementary Materials: The following supporting information can be downloaded at <https://www.mdpi.com/article/10.3390/cosmetics11030065/s1>, Figure S1: Content (mg/mL) of ingredients of LEO incorporated in CEL and NEL, one day after preparation (a) and after 30 days (b) and 60 days (c) of storage at 4 °C. Table S1: Percentage change in LEO content over time in CEL and NEL. Table S2: Skin hydration (arbitrary units) monitoring of each volunteer at every time point. Table S3: Monitoring of TEWL (g/m²/h) of each volunteer at every time point.

Author Contributions: Conceptualization, S.H. and F.N.L.; methodology, K.F. and V.D.D.; formal analysis, K.F. and V.D.D.; investigation, K.F.; data curation, K.F., V.D.D. and E.M.; writing—original draft preparation, S.H.; writing—review and editing, F.N.L., E.M. and K.A.; supervision, S.H. All authors have read and agreed to the published version of the manuscript.

Funding: This research received no external funding.

Institutional Review Board Statement: Ethical review and approval were waived for this study due to its noninvasive nature.

Informed Consent Statement: Informed consent was obtained from all subjects involved in the study.

Data Availability Statement: Data available upon request.

Conflicts of Interest: The authors declare no conflicts of interest.

References

1. Sarkic, A.; Stappen, I. Essential Oils and Their Single Compounds in Cosmetics—A Critical Review. *Cosmetics* **2018**, *5*, 11. [[CrossRef](#)]
2. Chircov, C.; Grumezescu, A.M. Chapter 6—Nanoemulsion preparation, characterization, and application in the field of biomedicine. In *Nanoarchitectonics in Biomedicine*; Grumezescu, A.M., Ed.; William Andrew Publishing: Norwich, NY, USA, 2019; pp. 169–188. [[CrossRef](#)]
3. Guzmán, E.; Lucia, A. Essential Oils and Their Individual Components in Cosmetic Products. *Cosmetics* **2021**, *8*, 114. [[CrossRef](#)]
4. Bunse, M.; Daniels, R.; Gründemann, C.; Heilmann, J.; Kammerer, D.R.; Keusgen, M.; Lindequist, U.; Melzig, M.F.; Morlock, G.E.; Schulz, H.; et al. Essential Oils as Multicomponent Mixtures and Their Potential for Human Health and WellBeing. *Front. Pharmacol.* **2022**, *13*, 956541. [[CrossRef](#)]
5. de Matos, S.P.; Lucca, L.G.; Koester, L.S. Essential oils in nanostructured systems: Challenges in preparation and analytical methods. *Talanta* **2019**, *1*, 204–214. [[CrossRef](#)] [[PubMed](#)]
6. Hatziantoniou, S.; Kapetanstratakis, I.S.; Drakoulis, N. Cosmetics and Personal Care Products. In *Encyclopedia of Toxicology*, 4th ed.; Philip, J.W., Ed.; Academic Press: Cambridge, MA, USA, 2024. [[CrossRef](#)]
7. de Groot, A.; Schmidt, E. Essential Oils, Part V: Peppermint Oil, Lavender Oil, and Lemongrass Oil. *Dermatitis* **2016**, *27*, 325–332. [[CrossRef](#)]
8. Cruz Sánchez, E.; García, M.T.; Pereira, J.; Oliveira, F.; Craveiro, R.; Paiva, A.; Gracia, I.; García-Vargas, J.M.; Duarte, A.R.C. Alginate–Chitosan Membranes for the Encapsulation of Lavender Essential Oil and Development of Biomedical Applications Related to Wound Healing. *Molecules* **2023**, *28*, 3689. [[CrossRef](#)]
9. Batiha, G.E.; Teibo, J.O.; Wasef, L.; Shaheen, H.M.; Akomolafe, A.P.; Teibo, T.K.A.; Al-Kuraishy, H.M.; Al-Garbeeb, A.I.; Alexiou, A.; Papadakis, M. A review of the bioactive components and pharmacological properties of Lavandula species. *Naunyn Schmiedeb. Arch. Pharmacol.* **2023**, *396*, 877–900. [[CrossRef](#)]
10. Dobros, N.; Zawada, K.D.; Paradowska, K. Phytochemical Profiling, Antioxidant and Anti-Inflammatory Activity of Plants Belonging to the Lavandula Genus. *Molecules* **2022**, *28*, 256. [[CrossRef](#)] [[PubMed](#)]
11. Yang, S.K.; Yusoff, K.; Thomas, W.; Akseer, R.; Alhosani, M.S.; Abushelaibi, A.; Lim, S.H.; Lai, K.S. Lavender essential oil induces oxidative stress which modifies the bacterial membrane permeability of carbapenemase producing *Klebsiella pneumoniae*. *Sci. Rep.* **2020**, *10*, 819. [[CrossRef](#)]
12. Sayout, A.; Ouarhach, A.; Rabie, R.; Dilagui, I.; Soraa, N.; Romane, A. Evaluation of Antibacterial Activity of Lavandulapedunculata subsp. atlantica (Braun-Blanq.) Romo Essential Oil and Selected Terpenoids against Resistant Bacteria Strains-Structure-Activity Relationships. *Chem. Biodivers.* **2020**, *17*, e1900496. [[CrossRef](#)]
13. D’Auria, F.D.; Tecca, M.; Strippoli, V.; Salvatore, G.; Battinelli, L.; Mazzanti, G. Antifungal activity of Lavandula angustifolia essential oil against Candida albicans yeast and mycelial form. *Med. Mycol.* **2005**, *43*, 391–396. [[CrossRef](#)] [[PubMed](#)]
14. Minooeianhaghighi, M.H.; Sepehrian, L.; Shokri, H. Antifungal effects of Lavandula binaludensis and Cuminum cyminum essential oils against Candida albicans strains isolated from patients with recurrent vulvovaginal candidiasis. *J. Mycol. Med.* **2017**, *27*, 65–71. [[CrossRef](#)] [[PubMed](#)]
15. Białoń, M.; Krzyśko-Łupicka, T.; Nowakowska-Bogdan, E.; Wieczorek, P.P. Chemical Composition of Two Different Lavender Essential Oils and Their Effect on Facial Skin Microbiota. *Molecules* **2019**, *24*, 3270. [[CrossRef](#)] [[PubMed](#)]
16. Ravi, T.P.U.; Padma, T. Nanoemulsions for drug delivery through different routes. *Res. Biotechnol.* **2011**, *2*, 1–13.
17. Ashaolu, T.J. Nanoemulsions for health, food, and cosmetics: A review. *Environ. Chem. Lett.* **2021**, *19*, 3381–3395. [[CrossRef](#)] [[PubMed](#)]
18. Solè, I.; Solans, C. Nanoemulsions. In *Encyclopedia of Colloid and Interface Science*; Tadros, T., Ed.; Springer: Berlin, Germany, 2013; pp. 733–747. [[CrossRef](#)]
19. Rabelo, C.A.S.; Taarji, N.; Khalid, N.; Kobayashi, I.; Nakajima, M.; Neves, M.A. Formulation and characterization of water-in-oil nanoemulsions loaded with açai berry anthocyanins: Insights of degradation kinetics and stability evaluation of anthocyanins and nanoemulsions. *Food Res. Int.* **2018**, *106*, 542–548. [[CrossRef](#)]
20. Cimino, C.; Maurel, O.M.; Musumeci, T.; Bonaccorso, A.; Drago, F.; Souto, E.M.B.; Pignatello, R.; Carbone, C. Essential Oils: Pharmaceutical Applications and Encapsulation Strategies into Lipid-Based Delivery Systems. *Pharmaceutics* **2021**, *13*, 327. [[CrossRef](#)] [[PubMed](#)]
21. Miastkowska, M.; Sikora, E.; Kulawik-Pióro, A.; Kantyka, T.; Bielecka, E.; Kałucka, U.; Kamińska, M.; Szulc, J.; Piasecka-Zelga, J.; Zelga, P.; et al. Bioactive Lavandula angustifolia essential oil-loaded nanoemulsion dressing for burn wound healing. In vitro and in vivo studies. *Biomater. Adv.* **2023**, *148*, 213362. [[CrossRef](#)] [[PubMed](#)]
22. Kazemi, M.; Mohammadifar, M.; Aghadavoud, E.; Vakili, Z.; Aarabi, M.H.; Talaei, S.A. Deep skin wound healing potential of lavender essential oil and licorice extract in a nanoemulsion form: Biochemical, histopathological and gene expression evidences. *J. Tissue Viability* **2020**, *29*, 116–124. [[CrossRef](#)]
23. Liakopoulou, A.; Mourelatou, E.; Hatziantoniou, S. Exploitation of traditional healing properties, using the nanotechnology’s advantages: The case of curcumin. *Toxicol. Rep.* **2021**, *28*, 1143–1155. [[CrossRef](#)]
24. Wolf, M.; Klang, V.; Stojcic, T.; Fuchs, C.; Wolzt, M.; Valenta, C. NLC versus nanoemulsions: Effect on physiological skin parameters during regular in vivo application and impact on drug penetration. *Int. J. Pharm.* **2018**, *549*, 343–351. [[CrossRef](#)] [[PubMed](#)]

25. de Sousa, D.P.; Damasceno, R.O.S.; Amorati, R.; Elshabrawy, H.A.; de Castro, R.D.; Bezerra, D.P.; Nunes, V.R.V.; Gomes, R.C.; Lima, T.C. Essential Oils: Chemistry and Pharmacological Activities. *Biomolecules* **2023**, *13*, 1144. [[CrossRef](#)] [[PubMed](#)]
26. Miladinović, D.L.; Dimitrijević, M.V.; Mihajlov-Krstev, T.M.; Marković, M.S.; Ćirić, V.M. The significance of minor components on the antibacterial activity of essential oil via chemometrics. *LWT* **2021**, *136*, 110305. [[CrossRef](#)]
27. Bera, B.; Khazal, R.; Schroën, K. Coalescence dynamics in oil-in-water emulsions at elevated temperatures. *Sci. Rep.* **2021**, *11*, 10990. [[CrossRef](#)]
28. Gordillo-Galeano, A.; Mora-Huertas, C.E. Hydrodynamic diameter and zeta potential of nanostructured lipid carriers: Emphasizing some parameters for correct measurements. *Colloids Surf. A Physicochem. Eng.* **2021**, *620*, 126610. [[CrossRef](#)]
29. Bruschi, M.L. Mathematical models of drug release. In *Strategies to Modify the Drug Release from Pharmaceutical Systems*; Woodhead Publishing: Cambridge, MA, USA, 2015; pp. 63–86. [[CrossRef](#)]
30. Korsmeyer, R.W.; Gurny, R.; Doelke, R.E.; Buri, P.; Peppas, N.A. Mechanisms of solute release from porous hydrophilic polymers. *Int. J. Pharm.* **1983**, *15*, 25–35. [[CrossRef](#)]
31. Peppas, N.A. Analysis of Fickian and non-Fickian drug release from polymers. *Pharm. Acta Helv.* **1985**, *60*, 110–111. Available online: <https://europepmc.org/article/MED/4011621> (accessed on 3 October 2023).
32. Ritger, P.L.; Peppas, N.A. A Simple Equation for Description of Solute Release I. Fickian and Non-Fickian Release from Non-Swellable Devices in the Form of Slabs, Spheres, Cylinders or Discs. *J. Control. Release* **1987**, *5*, 23–36. [[CrossRef](#)]
33. Dash, S.; Murthy, P.N.; Nath, L.; Chowdhury, P. Kinetic modeling on drug release from controlled drug delivery systems. *Acta Pol. Pharm.* **2010**, *67*, 217–223.
34. Vaz, S.; Silva, R.; Amaral, M.H.; Martins, E.; Sousa Lobo, J.M.; Silva, A.C. Evaluation of the biocompatibility and skin hydration potential of vitamin E-loaded lipid nanosystems formulations: In vitro and human in vivo studies. *Colloids Surf. B Biointerfaces* **2019**, *1*, 242–249. [[CrossRef](#)]
35. Infante, V.H.P.; Maia Campos, P.M.B.G.; Gaspar, L.R.; Darvin, M.E.; Schleusener, J.; Rangel, K.C.; Meinke, M.C.; Lademann, J. Safety and efficacy of combined essential oils for the skin barrier properties: In vitro, ex vivo and clinical studies. *Int. J. Cosmet. Sci.* **2022**, *44*, 118–130. [[CrossRef](#)] [[PubMed](#)]
36. Aqil, M.; Ahad, A.; Sultana, Y.; Ali, A. Status of terpenes as skin penetration enhancers. *Drug Discov. Today* **2007**, *12*, 1061–1067. [[CrossRef](#)] [[PubMed](#)]

Disclaimer/Publisher’s Note: The statements, opinions and data contained in all publications are solely those of the individual author(s) and contributor(s) and not of MDPI and/or the editor(s). MDPI and/or the editor(s) disclaim responsibility for any injury to people or property resulting from any ideas, methods, instructions or products referred to in the content.